



Geophysical Research Letters



RESEARCH LETTER

10.1029/2021GL094149

Key Points:

- On-shelf intrusions of ocean heat peak when the Antarctic Slope Current (ASC) weakens
- Synoptic scale ocean circulation dominantly controls the interannual variability of ASC strength
- Heat intrusions towards the Totten ice shelf are enhanced with upstream coastal freshening

Supporting Information:

Supporting Information may be found in the online version of this article.

Correspondence to:

Y. Nakayama,

 $Yoshihiro. Nakayama@lowtem.hokudai. \\ ac.jp$

Citation:

Nakayama, Y., Greene, C. A., Paolo, F. S., Mensah, V., Zhang, H., Kashiwase, H., et al. (2021). Antarctic Slope Current modulates ocean heat intrusions towards Totten Glacier. *Geophysical Research Letters*, 48, e2021GL094149. https://doi.org/10.1029/2021GL094149

Received 1 MAY 2021 Accepted 9 AUG 2021

© 2021. The Authors.

This is an open access article under the terms of the Creative Commons Attribution-NonCommercial-NoDerivs License, which permits use and distribution in any medium, provided the original work is properly cited, the use is non-commercial and no modifications or adaptations are made.

Antarctic Slope Current Modulates Ocean Heat Intrusions Towards Totten Glacier

Yoshihiro Nakayama¹, Chad A. Greene², Fernando S. Paolo², Vigan Mensah¹, Hong Zhang², Haruhiko Kashiwase³, Daisuke Simizu³, Jamin S. Greenbaum⁴, Donald D. Blankenship⁵, Ayako Abe-Ouchi⁶, and Shigeru Aoki¹

¹Institute of Low Temperature Science, Hokkaido University, Sapporo, Japan, ²Jet Propulsion Laboratory, California Institute of Technology, Pasadena, CA, USA, ³National Institute of Polar Research, Tachikawa, Japan, ⁴Scripps Institution of Oceanography, University of California, San Diego, La Jolla, CA, USA, ⁵Institute for Geophysics, University of Texas at Austin, Austin, TX, USA, ⁶Atmosphere and Ocean Research Institute, The University of Tokyo, Kashiwa, Japan

Abstract The Totten ice shelf (TIS) in East Antarctica has received increasing attention in recent years due to high basal melt rates, which have been linked to a presence of warm modified Circumpolar Deep Water (mCDW) observed at the ice front. We show that mCDW on-shelf intrusions towards the TIS strengthen when the Antarctic Slope Current (ASC) weakens. This demonstrates that the ASC has a blocking effect and ASC weakening leads to on-shelf intrusions, as proposed by previous observational studies. The interannual variability of the ASC is controlled primarily by atmospheric and oceanic conditions beyond our regional model domain. We further show that heat intrusions onto the continental shelf off the TIS are not influenced by off-shelf warming but are enhanced with coastal freshening, suggesting positive feedback whereby ice melt and freshening upstream could start a chain reaction, leading to increased melt, and further coastal freshening.

Plain Language Summary East Antarctica's Totten Glacier holds enough ice to raise global sea levels by more than 4 m, and it has recently been melting at an alarming rate. To understand what causes high melt rates at the base of Totten's floating ice shelf, we developed an ocean model that shows how warm water masses circulate throughout the region. We find that the westward-moving Antarctic Slope Current (ASC) has the ability to block warm water from flowing toward the Totten ice shelf. The warm ocean heat intrusions towards the Totten ice shelf are simulated in 1993–1994, 2004–2006, and 2015–2016 together with extreme ASC weakening events. The ASC strength in the interannual time scale, which caused these weakening events, is controlled primarily by atmospheric and oceanic processes that originate more than 1,000 km away. We also find that as upstream ocean freshens, the blocking effect of the slope current could weaken, setting up a feedback mechanism in which a weaker slope current and on-shelf freshening allows more warm water to access Totten, leading to increased melt, more on-shelf intrusions of warm water, and yet more melt, ad infinitum.

1. Introduction

The Totten Glacier (Figure 1), which holds an ice volume comparable to the entire marine-based West Antarctic Ice Sheet, is thinning and its grounding line is retreating (Greenbaum et al., 2015; Li et al., 2016; Rignot et al., 2019; Velicogna et al., 2014). On-shelf intrusions of modified Circumpolar Deep Water (mCDW) (Roberts et al., 2018; Silvano et al., 2018, 2019) are the primary driver of Totten ice shelf (TIS) melting; such intrusions have been observed flowing into the TIS cavity at a temperature of \sim 0.4°C (Rintoul et al., 2016).

The Antarctic Circumpolar Current is located in the deep waters (Figure 1) carrying CDW eastward (Jacobs, 1991; Orsi et al., 1995). Over the continental slope (Figure 1), the Antarctic Slope Current (ASC) flows westward (Thompson et al., 2018; Whitworth et al., 1985). Previous observational studies have suggested that atmospheric forcing and water mass characteristics over the shelf and the open ocean (e.g., Thompson et al., 2018) modifies Antarctic Slope Front (ASF) structures and modulates the ASC. For example, strong ASC is considered to act as a barrier to on-shelf ocean heat intrusions (Gill, 1973; Jacobs, 1991; Schmidtko et al., 2014; Thompson et al., 2018) from observational studies. However, for East Antarctic ice shelves, strong dynamical links between ASC and on-shelf mCDW intrusions have never been demonstrated.

NAKAYAMA ET AL. 1 of 10

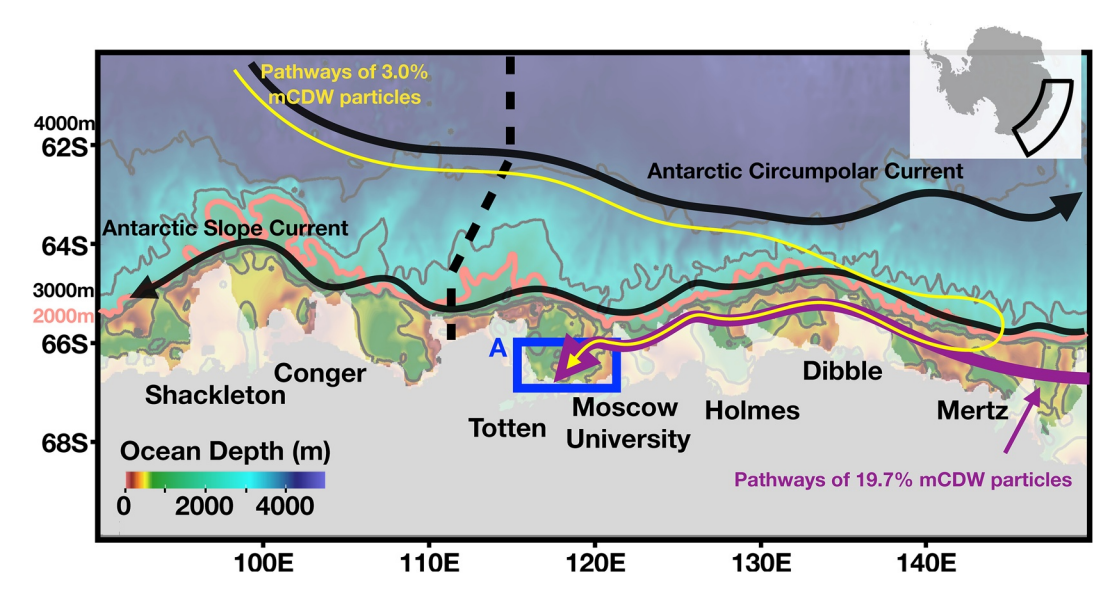


Figure 1. Model bathymetry (color) with black arrows indicating the Antarctic Circumpolar Current and Antarctic Slope Current as indicated in the figure. Bathymetric contours of 500, 1,000, 3,000, and 4,000 m are shown in gray and the bathymetric contour of 2,000 m is shown in pink. The inset (top right) shows Antarctica with the region surrounded by the black line denoting the model domain. Yellow and purple arrows indicate the pathways of particles onto the continental shelf off the Totten ice shelf (TIS) into box A enclosed by blue lines. The widths and sizes of these arrows represent that 19.7% of the particles at the TIS front originate from the continental shelf (shallower than 2,000 m) east of 125°E, and that 3.0% of particles originate from off-shelf waters deeper than 2,000 m. The black dashed line represents the vertical section shown in Figures S1 and S2.

Previous studies have investigated the impact of wind (Greene et al., 2017), sea-ice formation in upstream polynyas (Gwyther et al., 2014; Khazendar et al., 2013), cross-shelf ocean currents (Gwyther et al., 2014; Silvano et al., 2019) and ocean intrinsic variability (Gwyther et al., 2018) on the TIS melting. The mechanisms of mCDW intrusions, especially drivers of interannual changes, remain uncertain because time-varying estimates of ice shelf melt rates are only emerging now (Adusumilli et al., 2020) and long-term ocean observations to detect interannual changes are lacking.

In this study, we develop (a) a regional East Antarctic configuration of the Massachusetts Institute of Technology general circulation model (MITgcm) following (Nakayama et al., 2018) and (b) satellite estimates of temporally varying TIS melt rates (Figure 2a). We aim at understanding the drivers of interannual variability of mCDW on-shelf intrusions towards the TIS.

2. Methods and Experiments

2.1. Ocean Model Configuration

We use a regional configuration of the MITgcm with hydrostatic approximation, dynamic/thermodynamic sea-ice (Losch et al., 2010), and thermodynamic ice shelf (Losch, 2008) following (Nakayama et al., 2018) with horizontal grid spacing of 3–4 km and with 50 vertical levels (Figure 1) with some adjustments to model parameters (Table S1). Model bathymetry is based on the ETOPO1 (Amante & Eakins, 2012) with recent updates of more accurate bathymetry for the TIS region including data from Aurora (Rintoul et al., 2016), Shirase, and airborne gravity measurements acquired by the International Collaborative Exploration of the Cryosphere by Airborne Profiling project 7 (Figure 1). Model ice shelf draft is based on Antarctic Bedrock Mapping (Fretwell et al., 2013). We compute ice shelf melt rates following Hellmer and Olbers (1989), Holland and Jenkins (1999), and Jenkins (1991). We apply a permanent landfast ice mask based on Fraser et al. (2012). We conduct a 25-year model simulation from 1992 to 2016 (hereinafter CTRL) following a spin-up of 25 years. Atmospheric forcing is provided by ERA-Interim (Dee et al., 2011). Particle release and passive tracer experiments are conducted to analyze the circulation patterns of several water masses existing on the continental shelf (See method in Supporting Information S1 for detail).

NAKAYAMA ET AL. 2 of 10



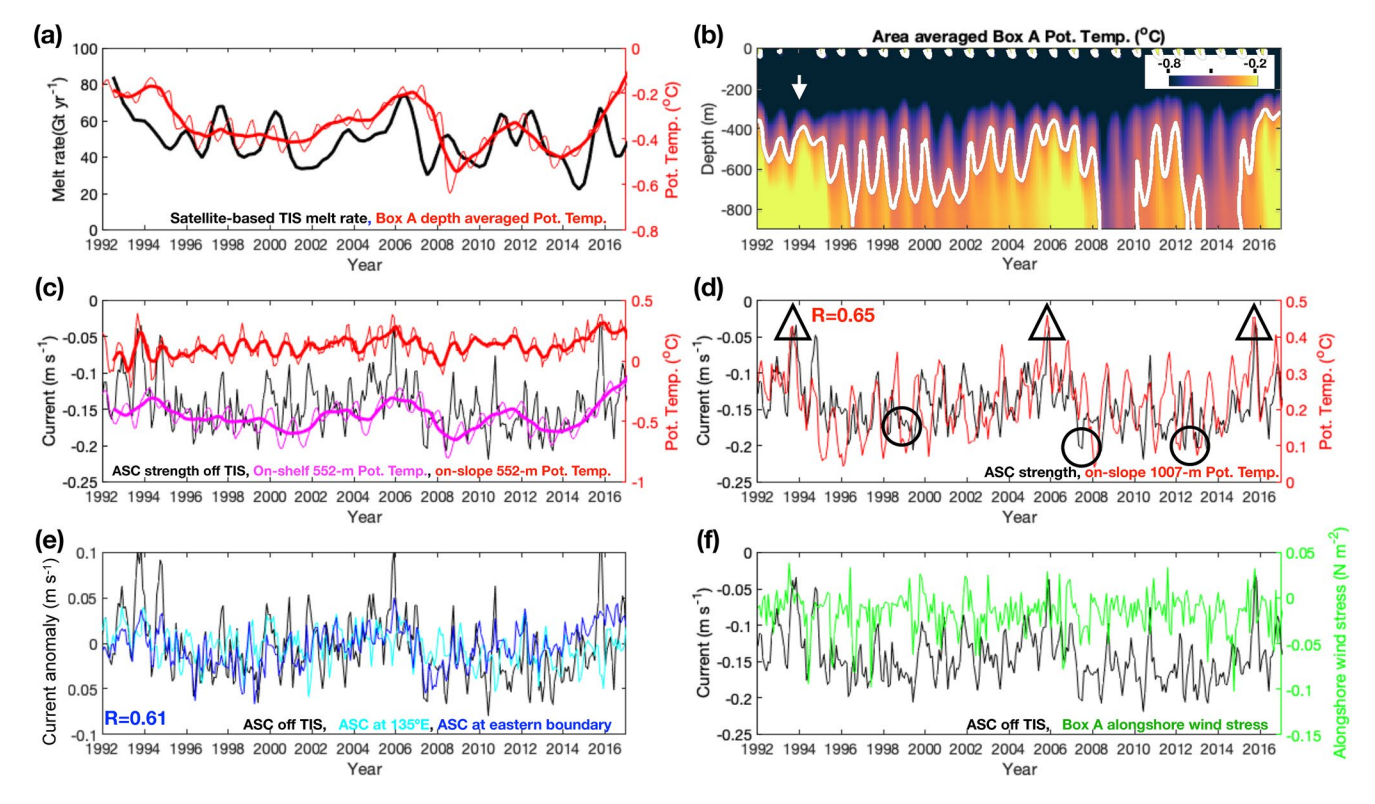


Figure 2. (a) Time series of satellite-based estimates of the Totten ice shelf melt rates (black) and box A depth averaged potential temperature between 514 and 918 m (red). (b) Times series of area-averaged box A potential temperature with a contour of -0.4°C (white). White arrow indicates the warm mCDW inflow in 1994. (c) Time series of box A potential temperature at 552 m depth (pink), potential temperature over the continental slope at 552 m depth (red), and Antarctic Slope Current (ASC) strength (positive eastward) at 552 m depth (black). Note that ASC is westward current. Properties over the continental slope are calculated as spatial averages along the 1,007-m isobath between 116.6°E and 121.6°E. For (a) and (c), thick lines indicate 12-month running averages. (d) Time series of the 552-m ASC strength (same as c, black) and 1,007-m potential temperature over the continental slope (red). Triangles and circles indicate strong and weak ASC years based on 552-m ASC strength in November. (e) Time series of 552-m ASC strength anomaly off the Totten ice shelf (TIS) (same as c, black) and at 135°E (cyan) and 1,007-m ASC strength at the eastern model boundary (blue). The ASC core is located deeper close to the eastern model boundary. The anomalies are calculated by subtracting temporal averages for each location. The value of correlation coefficients (*R*) are calculated using 12-month running means of ASC strengths off the TIS and at the eastern boundary. (f) Time series of ASC strength off the TIS (same as c, black) and alongshore wind stress over the bathymetric trough intruding mCDW towards the TIS (red box in Figure S6c).

2.2. Satellite Melt Rate Estimates

We derive ice shelf melt-rate time series from measurements acquired by four overlapping ESA satellite radar altimetry (RA) missions (Nilsson et al., 2016; Paolo et al., 2016 and supporting material for detail).

3. Results

Simulated horizontal and vertical sections capture large-scale hydrographic structures implying that large-scale ocean circulation is well represented in our simulations (Yamazaki et al., 2021, Figures S1–S4, and Model evaluation for detail). For the region on the continental shelf near the TIS front (box A in Figure 1), time series of spatial mean potential temperature show warm mCDW stored at depths below \sim 500 m and Winter Water located above (Figure 2b). As is common with ocean models (Gwyther et al., 2018), the simulated thermocline depth is shallower by a few hundred meters compared to observations (Rintoul et al., 2016; Silvano et al., 2017).

3.1. Simulated and Observed Interannual Variability

Near the TIS front (box A), the depth-averaged potential temperature between 514 and 918 m shows peaks of mCDW intrusions in 1994, 2006, 2011, and 2016 (Figure 2a). Satellite-based estimates of the TIS melt rates show similar interannual variability to the simulated depth-averaged potential temperature from the

NAKAYAMA ET AL. 3 of 10

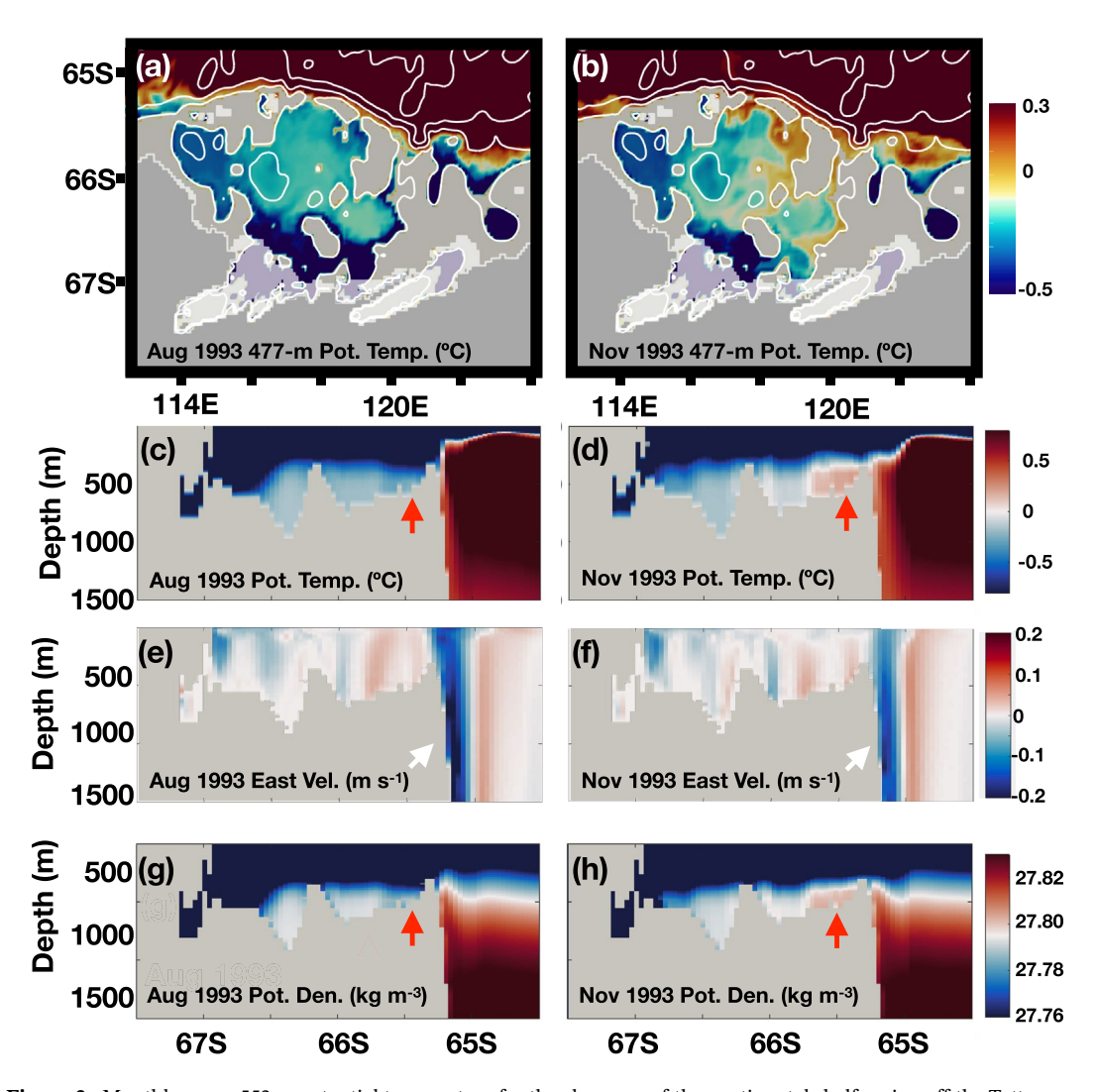


Figure 3. Monthly mean 552 m potential temperature for the close-ups of the continental shelf region off the Totten ice shelf in (a) August 1993 and (b) November 1993 for the CTRL case. Bathymetric contours of 500, 1,000, 2,000, 3,000, and 4,000 m are shown in white. Simulated vertical sections of (c and d) potential temperature, (e andf) eastward current, and (g and h) potential density along 119°E in August and November 1993 are shown, respectively. Red and white arrows highlight the simulated mCDW inflow and the changes in the Antarctic Slope Current strengths, respectively.

numerical model (Figure 2a). The satellite-based results indicate peak melt rates in 1992, 1997, 2000, 2006, 2011, 2012, and 2016; although not all of these peaks are found in the simulated results (e.g., 1997 and 2000), the largest peaks and the overall trend are common between the two time series. The simulated TIS melt rate also shows similar temporal variability but its peaks do not match exactly with mCDW intrusion peaks (Figure S5). This is, however, still in good agreement considering that (a) it is generally difficult for ocean models to reproduce interannual variability close to remote sensing observations, (b) knowledge of on-shelf bathymetry is only limited to the Dalton polynya and Totten ice shelf front with no bathymetric measurements available along the mCDW intrusions pathways, and (c) good representations of mCDW circulations require horizontal grid spacing of \sim 1 km (Nakayama, Timmermann, Schröder, & Hellmer, 2014; St-Laurent et al., 2013; Stewart & Thompson, 2016).

Sequential snapshots of 552-m on-shelf potential temperature describe a detailed view of the mCDW intrusions onto the continental shelf. For the mCDW intrusion peak during 1993–1994, for example, the intrusion (~0.4°C, Figure 2c) begins in September 1993 from two troughs existing along the continental shelf break and continues for several months before it weakens and stops (Figures 3a and 3b, Figure S6 (red and

NAKAYAMA ET AL. 4 of 10



magenta arrows), and Movie S1). Since on-shelf warming is caused by intrusions of warmer mCDW from the continental shelf break (Figure 2), simulated potential temperature time series over the continental slope and at the TIS front (box A) fluctuates similarly (Figure 2c). This is different from the case in the eastern Amundsen Sea where mCDW temperature shows little variability and volume change appears to control the available heat to melt ice shelves (Dutrieux et al., 2014; Kimura et al., 2017; Nakayama et al., 2019; Wåhlin et al., 2020; Webber et al., 2019).

3.2. What Induces Warm mCDW On-Shelf Intrusions?

To test whether the potential temperature of mCDW at TIS is modulated by large-scale ocean circulation as has been reported in the Amundsen Sea Embayment (Nakayama et al., 2018), we calculate the origin of mCDW by using particles released on the continental shelf near the TIS front, advected backward in time based on the daily output of ocean currents (Table S3 and Figures S7 and S8). Based on 14 experiments with different particle release years, we find from two years of backward integration that $19.7\pm3.6\%$ of the particles at the TIS front originate from the continental shelf region (shallower than 2,000 m) east of 125°E , and that $3.0\pm1.3\%$ of particles originate from off-shelf waters deeper than 2,000 m. Time series of the number of particles originating from the off-shelf region (Table S3) fluctuate similarly to mCDW on-shelf temperature (Figure 2b). However, the fluctuation is too little to explain the simulated interannual variability of on-shelf mCDW properties.

Of all simulated peaks of TIS front (box A) mCDW temperature, the warmest three cases accompany the extreme ASC weakening events (Figure 2c). For example, in 1993, the ASC weakens from August to November (white arrows in Figure 3), resulting in flattening of the isopycnal and on-shelf intrusions of mCDW in the following November (red arrows in Figure 3). The response is quick and warm mCDW intrudes on-shelf and it reaches the TIS front region within 4 months (Figure 3). This demonstrates that the ASC controls interannual variability of mCDW intrusions and strong ASC acts as a barrier to on-shelf ocean heat intrusions (Figure 2c) as suggested from previous observational studies (Gill, 1973; Jacobs, 1991; Schmidtko et al., 2014; Thompson et al., 2018).

3.3. What Controls the ASC Strengths?

The ASC generally responds to wind, large-scale modes of climate variability (e.g., El Niño, Southern Annular Mode, etc), and dense shelf water descent upstream along the Antarctic coast (Gill, 1973; Mathiot et al., 2011; Marques et al., 2014; Nakayama, Ohshima, et al., 2014; Peña-Molino et al., 2016; Stewart & Thompson, 2015; Thompson et al., 2018). Using 12-month running averages, we find a high and significant correlation (r = 0.61, Figure 2e) between the 552-m ASC strength off the TIS and the 1,007-m ASC strength at the eastern model boundary. No significant correlation can be found between the ASC strength and alongshore wind close to the continental shelf break (Figure 2f).

Based on the high correlations between the ASC strength off the TIS and at the eastern model boundary, we find that the interannual variability of mCDW intrusions and ASC strength is primarily due to the interannual variability of the ASC at the eastern ocean lateral boundary. This implies that large-scale atmospheric and ocean circulations outside of the model domain control the ASC strength. However, the ASC weakening events (e.g., 1993–1994, 2004–2006, and 2015–2016) do not occur at the exact same time in different locations (Figure 2e). This means that the background ASC strength provides favorable conditions for the mCDW intrusions but local ocean processes are able to influence the ASC strength and mCDW intrusions onto the continental shelf (Figure 2e).

Although the simulated ASC weakening events off the TIS in 1993, 2005, and 2015 are prominent (ASC strength weakens by \sim 0.15 m s⁻¹), ASC strengths at other locations show small fluctuations (Figure 2e). This means that local processes inside of the model domain induce amplified ASC weakening off the TIS. As ASC weakening is prominent from October to November, we select six years with weak (1993, 2005, and 2015) and strong ASC (1998, 2007, and 2012) based on November monthly averages (marked by triangles and circles, respectively, in Figure 2d) and compare composite of November mean vertical sections of potential temperature, eastward ocean current, and passive tracer concentration (Figure 4). The passive tracer concentration is below 0.1 everywhere in the region deeper than 500 m for weak ASC years (Figure 4e and

NAKAYAMA ET AL. 5 of 10

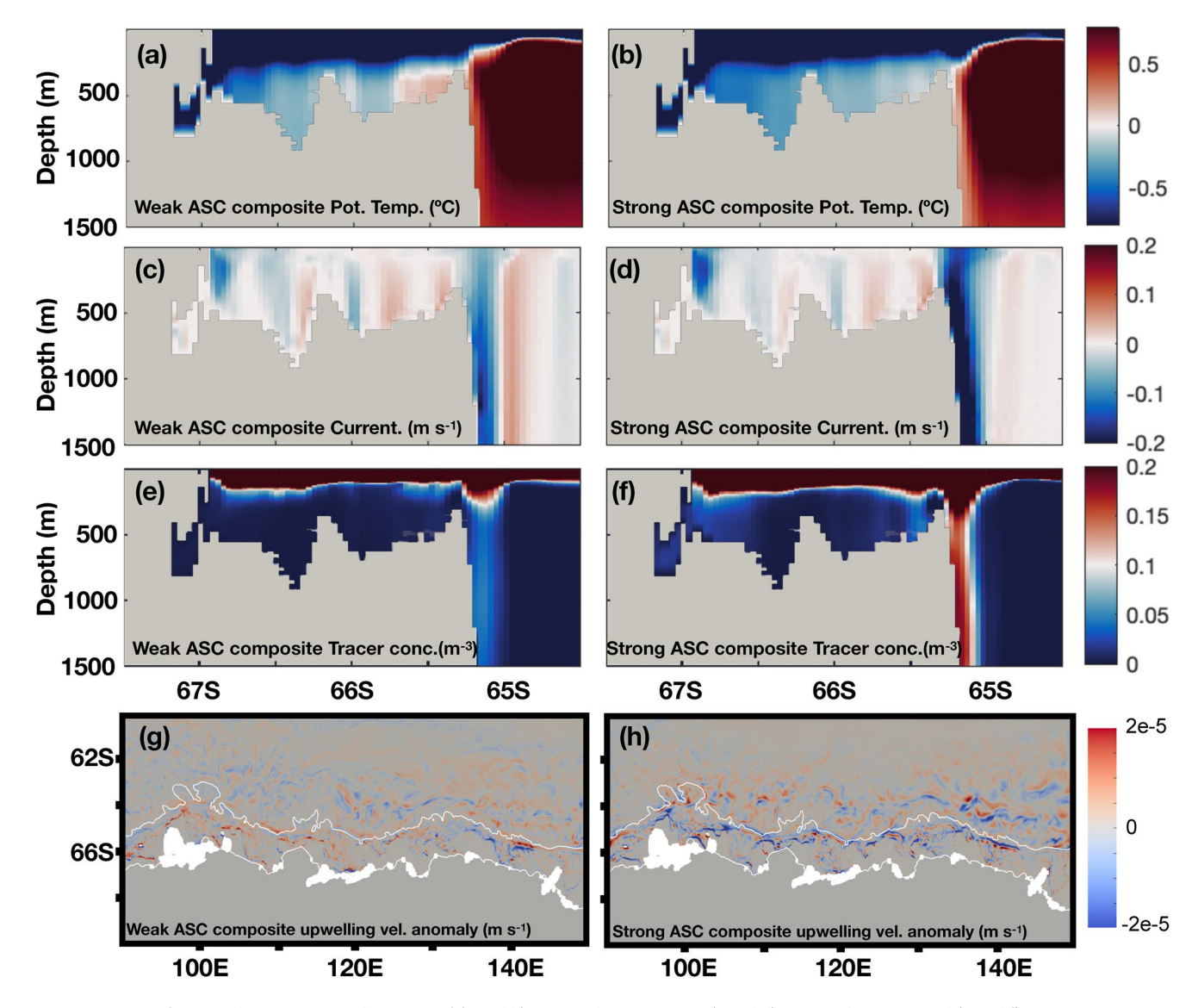


Figure 4. Composite of November mean vertical sections of (a and b) potential temperature, (c and d) eastward current, and (e and f) passive tracer concentration along 119°E for weak and strong Antarctic Slope Current (ASC) years. Strong and weak ASC years are sampled based on the ASC strength in November (Figure 2d). Spatial distribution of nine-month (September–November for all sampled years) mean Ekman upwelling for (g) weak and (h) strong ASC years. Bathymetric contours of 0 and 2,000 m are shown in white.

Figure S9), while passive tracer concentration is high throughout the water column over the continental slope with local maximum passive tracer concentration of \sim 0.18 located at the bottom over the continental slope for strong ASC years. Vertically stretched distribution of the passive tracer, high tracer concentration at the bottom, and the emergence of low-temperature water together with ASC strengthening (Figures 2d and 4) imply that downslope descent of shelf water onto the continental slope upstream causes stretching of the water column and strengthening of the ASC (Lane-Serff & Baines, 1998). This can be also confirmed from the high and significant correlation (r = 0.65) between 12-months running means of ASC strength and the ASC temperature at 1,007 m depth (Figure 2d). The simulated ASC cores are located at similar locations for both strong and weak ASC cases.

Another major difference can be found over the slope in upwelling velocity estimated from surface ocean stress (Figures 4g and 4h). The spatially averaged upwelling velocities are 2.1×10^{-6} m s⁻¹ and -2.0×10^{-7} m s⁻¹ for the continental slope region (spatially averaged for the area between 115° and 121.6°E and depth

NAKAYAMA ET AL. 6 of 10



between 1,000 m and 2,000 m), respectively, for weak and strong ASC years (Figures 4g and 4h and Figure S10), consistent with Greene et al. (2017). This likely means that coastal upwelling modifies ASF structure, modifies ASC strengths, and controls mCDW on-shelf intrusions (Webber et al., 2019). We do not find a clear distinction for alongshore wind between strong and weak ASC years (Figure S10).

Similar relations between the ASC strength and 552-m potential temperature along the 1,000-m isobath can be found off the Shackleton, Holmes, and Dibble ice shelves (Figure S11). The correlation coefficients between the ASC strength and 550-m potential temperature are 0.46 and 0.49, respectively, for the region off the Shackleton and Dibble ice shelves, implying some robustness of the dynamical link between ASC weakening and cross-shelf mCDW flow. For example, on-shelf mCDW temperature off the Shackleton Ice Shelf is high between 2004 and 2008 when the ASC is weak, showing a consistent behavior.

In our simulations, we show that the ASC has a blocking effect, and weakening of the ASC leads to intrusions of warm mCDW onto the continental shelf towards the TIS front. Our model shows larger interannual fluctuations in the temperature of the mCDW layer compared to previous studies (Gwyther et al., 2014, 2018; Khazendar et al., 2013; Silvano et al., 2019), likely because the model bathymetry in previous studies included a deep, wide trough that allowed the ASC to approach the TIS front. We note that we use a regional model to investigate large-scale thermal exchange across the continental shelf, so our analysis focuses on the delivery of thermal energy towards the TIS. We do not attempt to resolve fine-scale circulations beneath TIS or any polynya-driven processes that may affect melt rates at TIS (Gwyther et al., 2014; Khazendar et al., 2013). Our results do not contradict the overall findings of any previous study, but add a layer of complexity to our understanding of the forcing mechanisms that drive interannual thermal variability in the region surrounding TIS.

3.4. Sensitivity to Shelf Water Freshening and Off-Shelf CDW Warming

We conduct additional experiments (Table S2) to investigate the sensitivity of the on-shelf heat content (box A in Figure 1) to off-shelf CDW warming and shelf water freshening, which are comparable to ongoing changes observed in the Southern Ocean (Böning et al., 2008; Jacobs et al., 2002; Rye et al., 2014; Schmidtko et al., 2014). Neither off-shelf mCDW warming (Warm1 and Warm2) nor enhanced air-ice drag coefficient (Wind2) significantly influences on-shelf mCDW temperature (Figure 5). However, imposed on-shelf freshening at the eastern model boundary (Figure S12) leads to warming of the on-shelf mCDW. On-shelf freshening by 0.1 and 0.2 leads to on-shelf warming by 0.04 °C and 0.3°C, respectively, showing a nonlinear response (Figure 5). Such changes occur because the density reduction of on-shelf properties leads to intensified and more frequent intrusions of mCDW towards the TIS at the time when ASC weakens (Figure S13). The simulated ASC also weakens by 11% and 36%, respectively, for Fresh1 and Fresh2 experiments, which possibly intensifies on-shelf warming (Figure S13). These sensitivity experiments further confirm the importance of freshening on ASC and on-shelf mCDW intrusions in addition to on-shelf convective processes (e.g., Silvano et al., 2018). These results have to be understood carefully as recent studies are suggesting both strengthening and weakening trends for future ASC (Moorman et al., 2020; Pelle et al., 2021). Circum-Antarctic or global high-resolution ocean simulations are required for studying future ASC response, because ASC is likely sensitive to circum-Antarctic on-shelf conditions and ice shelf melting (Graham et al., 2013; Moorman et al., 2020; Nakayama, Timmermann, Rodehacke, et al., 2014; Thompson et al., 2018).

4. Conclusions

We show that simulated ocean heat intrusions towards the TIS present several peaks in 1994, 2006, 2011, and 2016, consistent with satellite-based estimates (Figure 2). We demonstrate that the ASC plays a role in blocking ocean heat intrusions towards the TIS under the realistic East Antarctic region configuration. The interannually varying strength of the ASC is primarily controlled by lateral ocean boundary conditions (and thus large-scale atmospheric and ocean circulation outside of model domain), but also likely influenced by local wind stress curl and upstream descent of shelf water. On-shelf intrusions of mCDW toward the TIS is sensitive to shelf water freshening, such that a 0.2 decrease in salinity leads to a 19% increase of on-shelf heat content compared to CTRL, but off-shelf warming does not influence on-shelf mCDW temperature (Figure 5), indicating that ongoing Antarctic coastal freshening (Jacobs et al., 2002; Nakayama et al., 2020;

NAKAYAMA ET AL. 7 of 10

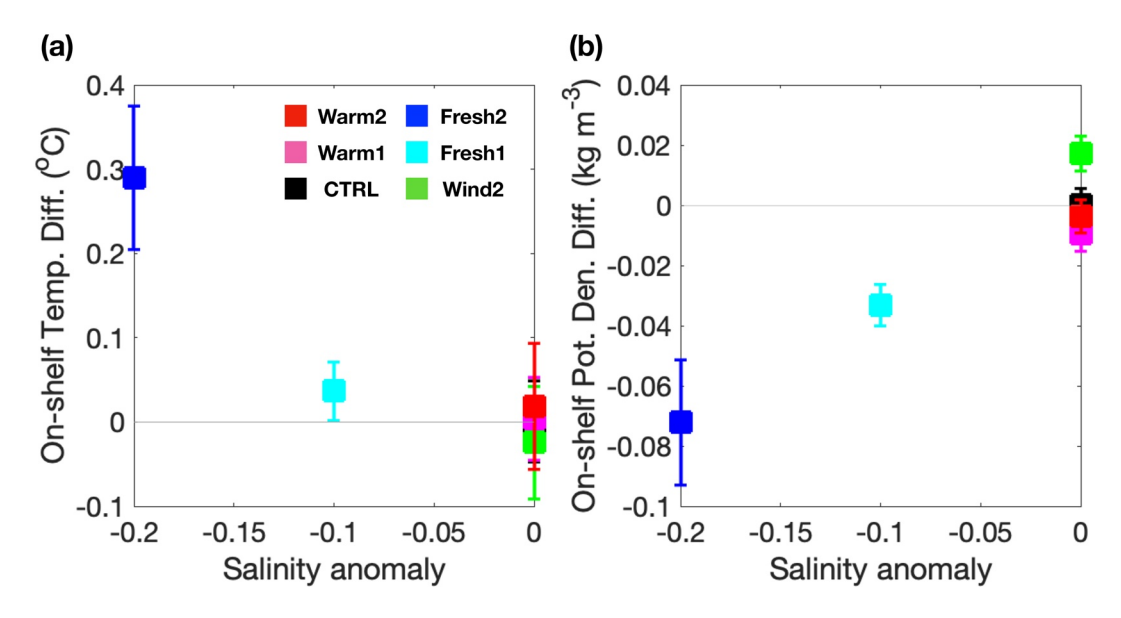


Figure 5. Sensitivities of (a) on-shelf potential temperature and (b) on-shelf potential density differences to freshening at the eastern model boundary, off-shelf CDW warming, and enhanced air-ice drag coefficient. The *x*-axis indicates salinity anomaly showing on-shelf salinity difference at the eastern boundary compared to CTRL. Standard deviations of potential temperature and potential density during warm periods (1994–1995 and 2006–2008) are calculated for each sensitivity experiment (shown as error bars). On-shelf properties are defined as spatial averages in box A at 552 m depth.

Rye et al., 2014) may have already accelerated the melting of the TIS. Due to the large-scale nature of the continental slope processes that drive the ASC, it is probable that the relationship between ASC strength and coastal ocean heat may influence other East Antarctic ice shelves in addition to TIS.

Data Availability Statement

The model code, input, and results are available at https://doi.org/10.5281/zenodo.5077265. They are also available at https://ecco.jpl.nasa.gov/drive/files/ECCO2/LatLon_East_Antarctic. Some of the figures are created using Paraview and Ocean Data View.

References

Adusumilli, S., Fricker, H. A., Medley, B., Padman, L., & Siegfried, M. R. (2020). Interannual variations in meltwater input to the Southern Ocean from Antarctic ice shelves. *Nature Geoscience*, 13(9), 616–620. https://doi.org/10.1038/s41561-020-0616-z

Amante, C., & Eakins, B. (2012). Etopo1, global 1 arc-minute ocean depth and land elevation from the US National Geophysical Data Center (NGDC).

Böning, C. W., Dispert, A., Visbeck, M., Rintoul, S., & Schwarzkopf, F. U. (2008). The response of the Antarctic Circumpolar Current to recent climate change. *Nature Geoscience*, 1(12), 864–869. https://doi.org/10.1038/ngeo362

Dee, D., Uppala, S., Simmons, A., Berrisford, P., Poli, P., Kobayashi, S., et al. (2011). The ERA-Interim reanalysis: Configuration and performance of the data assimilation system. *Quarterly Journal of the Royal Meteorological Society*, 137(656), 553–597.

Dutrieux, P., De Rydt, J., Jenkins, A., Holland, P. R., Ha, H. K., Lee, S. H., et al. (2014). Strong sensitivity of Pine Island ice-shelf melting to climatic variability. *Science*, 343(6167), 174–178. https://doi.org/10.1126/science.1244341

Fraser, A. D., Massom, R. A., Michael, K. J., Galton-Fenzi, B. K., & Lieser, J. L. (2012). East Antarctic landfast sea ice distribution and variability, 2000–08. Journal of Climate, 25(4), 1137–1156. https://doi.org/10.1175/jcli-d-10-05032.1

Fretwell, P., Pritchard, H. D., Vaughan, D. G., Bamber, J., Barrand, N., Bell, R., et al. (2013). Bedmap2: Improved ice bed, surface and thickness datasets for Antarctica. *The Cryosphere*, 7(1), 375–393.

Gill, A. (1973). Circulation and bottom water production in the Weddell Sea. Deep Sea Research and Oceanographic Abstracts, 20, 111–140. https://doi.org/10.1016/0011-7471(73)90048-x

Graham, J. A., Heywood, K. J., Chavanne, C. P., & Holland, P. R. (2013). Seasonal variability of water masses and transport on the Antarctic continental shelf and slope in the southeastern Weddell Sea. *Journal of Geophysical Research: Oceans*, 118(4), 2201–2214. https://doi.org/10.1002/jgrc.20174

Greenbaum, J., Blankenship, D., Young, D., Richter, T., Roberts, J., Aitken, A., et al. (2015). Ocean access to a cavity beneath Totten Glacier in East Antarctica. *Nature Geoscience*, 8(4), 294–298. https://doi.org/10.1038/ngeo2388

Greene, C. A., Blankenship, D. D., Gwyther, D. E., Silvano, A., & van Wijk, E. (2017). Wind causes Totten Ice Shelf melt and acceleration. Science Advances, 3(11), e1701681. https://doi.org/10.1126/sciadv.1701681

Acknowledgments

Simulations were carried out at the University of Tokyo Supercomputing facilities. We thank Kaihe Yamazaki, Alessandro Silvano, Daisuke Hirano, Xichen Li, and Kay I. Ohshima for their useful comments and suggestions. We also thank the officers, crew, and scientists on board Aurora Australis (2015) and Icebreaker Shirase (JARE58 and 59). This work was supported by Grants-in-Aids for Scientific Research (19K23447, 21K13989, 17H01615, 17H06322, 17H06104, 21H04918, and 21H01201) from the Ministry of Education, Culture, Sports, Science, and Technology in Japan. The authors also acknowledge funding from MEXT KAKENHI grant 17H06323; J.S.G. was supported by NSF OPP-2114454; D.D.B. was supported by the G. Unger Vetlesen Foundation. Insightful comments from the two anonymous reviewers were very helpful for improvement of the manuscript.

NAKAYAMA ET AL. 8 of 10



- Gwyther, D., Galton-Fenzi, B., Hunter, J., & Roberts, J. (2014). Simulated melt rates for the Totten and Dalton ice shelves. *Ocean Science*, 10(3), 267–279. https://doi.org/10.5194/os-10-267-2014
- Gwyther, D., O'Kane, T. J., Galton-Fenzi, B. K., Monselesan, D. P., & Greenbaum, J. S. (2018). Intrinsic processes drive variability in basal melting of the Totten Glacier ice shelf. *Nature Communications*, 9(1), 1–8. https://doi.org/10.1038/s41467-018-05618-2
- Hellmer, H., & Olbers, D. (1989). A two-dimensional model for the thermohaline circulation under an ice shelf. *Antarctic Science*, 1(4), 325–336. https://doi.org/10.1017/s0954102089000490
- Holland, D. M., & Jenkins, A. (1999). Modeling thermodynamic ice-ocean interactions at the base of an ice shelf. *Journal of Physical Ocean-ography*, 29(8), 1787–1800. https://doi.org/10.1175/1520-0485(1999)029<1787:mtioia>2.0.co;2
- Jacobs, S. S. (1991). On the nature and significance of the Antarctic Slope Front. Marine Chemistry, 35(1-4), 9-24. https://doi.org/10.1016/s0304-4203(09)90005-6
- Jacobs, S. S., Giulivi, C. F., & Mele, P. A. (2002). Freshening of the Ross Sea during the late 20th century. Science, 297(5580), 386–389. https://doi.org/10.1126/science.1069574
- Jenkins, A. (1991). A one-dimensional model of ice shelf-ocean interaction. *Journal of Geophysical Research*, 96(C11), 20671–20677. https://doi.org/10.1029/91jc01842
- Khazendar, A., Schodlok, M., Fenty, I., Ligtenberg, S., Rignot, E., & Van Den Broeke, M. (2013). Observed thinning of Totten Glacier is linked to coastal polynya variability. *Nature Communications*, 4(1), 1–9. https://doi.org/10.1038/ncomms3857
- Kimura, S., Jenkins, A., Regan, H., Holland, P. R., Assmann, K. M., Whitt, D. B., et al. (2017). Oceanographic controls on the variability of ice-shelf basal melting and circulation of glacial meltwater in the Amundsen Sea Embayment, Antarctica. *Journal of Geophysical Research: Oceans*, 122(12), 10131–10155. https://doi.org/10.1002/2017jc012926
- Lane-Serff, G. F., & Baines, P. G. (1998). Eddy formation by dense flows on slopes in a rotating fluid. *Journal of Fluid Mechanics*, 363, 229–252. https://doi.org/10.1017/s0022112098001013
- Li, X., Rignot, E., Mouginot, J., & Scheuchl, B. (2016). Ice flow dynamics and mass loss of Totten Glacier, East Antarctica, from 1989 to 2015. *Geophysical Research Letters*, 43(12), 6366–6373. https://doi.org/10.1002/2016gl069173
- Losch, M. (2008). Modeling ice shelf cavities in a z coordinate ocean general circulation model. *Journal of Geophysical Research*, 113(C8), C08043. https://doi.org/10.1029/2007jc004368
- Losch, M., Menemenlis, D., Heimbach, P., Campin, J.-M., & Hill, C. (2010). On the formulation of sea-ice models. Part 1: Effects of different solver implementations and parameterizations. *Ocean Modelling*, 33, 129–144. https://doi.org/10.1016/j.ocemod.2009.12.008
- Marques, G. M., Padman, L., Springer, S. R., Howard, S. L., & Özgökmen, T. M. (2014). Topographic vorticity waves forced by Antarctic dense shelf water outflows. Geophysical Research Letters, 41(4), 1247–1254. https://doi.org/10.1002/2013gl059153
- Mathiot, P., Goosse, H., Fichefet, T., Barnier, B., & Gallée, H. (2011). Modelling the seasonal variability of the Antarctic slope current. Ocean Science, 7(4), 455–470. https://doi.org/10.5194/os-7-455-2011
- Moorman, R., Morrison, A. K., & McC Hogg, A. (2020). Thermal responses to Antarctic ice shelf melt in an eddy-rich global ocean–sea ice model. *Journal of Climate*, 33(15), 6599–6620. https://doi.org/10.1175/jcli-d-19-0846.1
- Nakayama, Y., Manucharayan, G., Kelin, P., Torres, H. G., Schodlok, M., Rignot, E., & Menemenlis, D. (2019). Pathway of circumpolar deep water into Pine Island and Thwaites ice shelf cavities and to their grounding lines. Scientific Reports, 9, 16649.
- Nakayama, Y., Menemenlis, D., Zhang, H., Schodlok, M., & Rignot, E. (2018). Origin of circumpolar deep water intruding onto the Amundsen and Bellingshausen Sea continental shelves. *Nature Communications*, 9(1), 1–9. https://doi.org/10.1038/s41467-018-05813-1
- Nakayama, Y., Olshima, K. I., Matsumura, Y., Fukamachi, Y., & Hasumi, H. (2014). A numerical investigation of formation and variability of Antarctic bottom water off Cape Darnley, East Antarctica. *Journal of Physical Oceanography*, 44(11), 2921–2937. https://doi.org/10.1175/jpo-d-14-0069.1
- Nakayama, Y., Timmermann, R., & Hellmer, H. (2020). Impact of west Antarctic ice shelf melting on southern ocean hydrography. *The Cryosphere*, 14(7), 2205–2216. https://doi.org/10.5194/tc-14-2205-2020
- Nakayama, Y., Timmermann, R., Rodehacke, C. B., Schröder, M., & Hellmer, H. H. (2014). Modeling the spreading of glacial meltwater from the Amundsen and Bellingshausen Seas. *Geophysical Research Letters*, 41(22), 7942–7949. https://doi.org/10.1002/2014gl061600
- Nakayama, Y., Timmermann, R., Schröder, M., & Hellmer, H. (2014). On the difficulty of modeling circumpolar deep water intrusions onto the Amundsen Sea continental shelf. *Ocean Modelling*, 84, 26–34. https://doi.org/10.1016/j.ocemod.2014.09.007
- Nilsson, J., Gardner, A., Sandberg Sørensen, L., & Forsberg, R. (2016). Improved retrieval of land ice topography from CryoSat-2 data and its impact for volume-change estimation of the Greenland Ice Sheet. *The Cryosphere*, 10(6), 2953–2969. https://doi.org/10.5194/tc-10-2953-2016
- Orsi, A. H., Whitworth, T., III, & Nowlin, W. D., Jr. (1995). On the meridional extent and fronts of the Antarctic Circumpolar Current. Deep Sea Research Part I: Oceanographic Research Papers. 42(5), 641–673, https://doi.org/10.1016/0967-0637(95)00021-w
- Paolo, F. S., Fricker, H. A., & Padman, L. (2016). Constructing improved decadal records of Antarctic ice shelf height change from multiple satellite radar altimeters. *Remote Sensing of Environment*, 177, 192–205. https://doi.org/10.1016/j.rse.2016.01.026
- Peña-Molino, B., McCartney, M., & Rintoul, S. (2016). Direct observations of the Antarctic Slope Current transport at 113°e. *Journal of Geophysical Research: Oceans*, 121(10), 7390–7407. https://doi.org/10.1002/2015jc011594
- Pelle, T., Morlighem, M., Nakayama, Y., & Serrousi, H. (2021). Widespread grounding line retreat of Totten Glacier over the 21st century. Geophysical Research Letters, 48, e2021GL093213. https://doi.org/10.1029/2021GL093213
- Rignot, E., Mouginot, J., Scheuchl, B., van den Broeke, M., van Wessem, M. J., & Morlighem, M. (2019). Four decades of Antarctic Ice Sheet mass balance from 1979–2017. *Proceedings of the National Academy of Sciences of the United States of America*, 116(4), 1095–1103. https://doi.org/10.1073/pnas.1812883116
- Rintoul, S. R., Silvano, A., Pena-Molino, B., van Wijk, E., Rosenberg, M., Greenbaum, J. S., & Blankenship, D. D. (2016). Ocean heat drives rapid basal melt of the Totten Ice Shelf. Science Advances, 2(12), e1601610. https://doi.org/10.1126/sciadv.1601610
- Roberts, J., Galton-Fenzi, B. K., Paolo, F. S., Donnelly, C., Gwyther, D. E., Padman, L., et al. (2018). Ocean forced variability of Totten Glacier mass loss. Geological Society, London, Special Publications, 461(1), 175–186. https://doi.org/10.1144/sp461.6
- Rye, C. D., Garabato, A. C. N., Holland, P. R., Meredith, M. P., Nurser, A. G., Hughes, C. W., et al. (2014). Rapid sea-level rise along the Antarctic margins in response to increased glacial discharge. *Nature Geoscience*, 7(10), 732–735. https://doi.org/10.1038/ngeo2230
- Schmidtko, S., Heywood, K. J., Thompson, A. F., & Aoki, S. (2014). Multidecadal warming of Antarctic waters. Science, 346(6214), 1227–1231. https://doi.org/10.1126/science.1256117
- Silvano, A., Rintoul, S. R., Kusahara, K., Peña-Molino, B., van Wijk, E., Gwyther, D. E., & Williams, G. D. (2019). Seasonality of warm water intrusions onto the continental shelf near the Totten Glacier. *Journal of Geophysical Research: Oceans*, 124(6), 4272–4289. https://doi.org/10.1029/2018jc014634

NAKAYAMA ET AL. 9 of 10



- Silvano, A., Rintoul, S. R., Peña-Molino, B., Hobbs, W. R., van Wijk, E., Aoki, S., & Williams, G. D. (2018). Freshening by glacial meltwater enhances melting of ice shelves and reduces formation of Antarctic Bottom Water. *Science Advances*, 4(4), eaap9467. https://doi.org/10.1126/sciadv.aap9467
- Silvano, A., Rintoul, S. R., Peña-Molino, B., & Williams, G. D. (2017). Distribution of water masses and meltwater on the continental shelf near the Totten and Moscow University ice shelves. *Journal of Geophysical Research: Oceans*, 122(3), 2050–2068. https://doi.org/10.1002/2016jc012115
- Stewart, A. L., & Thompson, A. F. (2015). Eddy-mediated transport of warm circumpolar deep water across the Antarctic Shelf Break. Geophysical Research Letters, 42(2), 432–440. https://doi.org/10.1002/2014gl062281
- Stewart, A. L., & Thompson, A. F. (2016). Eddy generation and jet formation via dense water outflows across the Antarctic continental slope. *Journal of Physical Oceanography*, 46(12), 3729–3750. https://doi.org/10.1175/jpo-d-16-0145.1
- St-Laurent, P., Klinck, J. M., & Dinniman, M. S. (2013). On the role of coastal troughs in the circulation of warm circumpolar deep water on Antarctic Shelves. *Journal of Physical Oceanography*, 43(1), 51–64. https://doi.org/10.1175/jpo-d-11-0237.1
- Thompson, A. F., Stewart, A. L., Spence, P., & Heywood, K. J. (2018). The Antarctic Slope Current in a changing climate. *Reviews of Geophysics*, 56(4), 741–770. https://doi.org/10.1029/2018rg000624
- Velicogna, I., Sutterley, T., & Van Den Broeke, M. (2014). Regional acceleration in ice mass loss from Greenland and Antarctica using GRACE time-variable gravity data. *Geophysical Research Letters*, 41(22), 8130–8137. https://doi.org/10.1002/2014gl061052
- Wåhlin, A. K., Steiger, N., Darelius, E., Assmann, K. M., Glessmer, M. S., Ha, H. K., et al. (2020). Ice front blocking of ocean heat transport to an Antarctic ice shelf. *Nature*, 578(7796), 568–571. https://doi.org/10.1038/s41586-020-2014-5
- Webber, B. G., Heywood, K. J., Stevens, D. P., & Assmann, K. M. (2019). The impact of overturning and horizontal circulation in Pine Island Trough on ice shelf melt in the eastern Amundsen Sea. *Journal of Physical Oceanography*, 49(1), 63–83. https://doi.org/10.1175/jpo-d-17-0213.1
- Whitworth, T., III, Orsi, A., Kim, S.-J., Nowlin, W., Jr., & Locarnini, R. (1985). Water masses and mixing near the Antarctic Slope Front. Ocean, ice, and atmosphere: interactions at the Antarctic continental margin, 75, 1–27.
- Yamazaki, K., Aoki, S., Katsumata, K., Hirano, D., & Nakayama, Y. (2021). Multidecadal poleward shift of the southern boundary of the Antarctic Circumpolar Current off East Antarctica. Science Advances, 7(24), eabf8755. https://doi.org/10.1126/sciadv.abf8755

References From the Supporting Information

- Adusumilli, S., Fricker, H. A., Siegfried, M. R., Padman, L., Paolo, F. S., & Ligtenberg, S. R. (2018). Variable basal melt rates of Antarctic Peninsula ice shelves, 1994–2016. *Geophysical Research Letters*, 45(9), 4086–4095. https://doi.org/10.1002/2017gl076652
- Antonov, J. I., Seidov, D., Boyer, T. P., Locarnini, R. A., Mishonov, A. V., Garcia, H. E., & Johnson, D. R. (2010). World Ocean Atlas 2009, Volume 2: Salinity. Washington, DC. In S. Levitus (Ed.), NOAA Atlas NESDIS 69, U.S. Government Printing Office.
- Cavalieri, D., Parkinson, C., Gloersen, P., & Zwally, H. (2006). Sea ice concentrations from Nimbus-7 SMMR and DMSP SSM/I passive microwave data. January 1979–June 2006.
- Gouretski, V. (2018). World ocean circulation experiment–argo global hydrographic climatology. Ocean Science, 14(5), 1127–1146. https://doi.org/10.5194/os-14-1127-2018
- Locarnini, R. A., Mishonov, A. V., Antonov, J. I., Boyer, T. P., & Garcia, H. E. (2010). World Ocean Atlas 2009, Volume 1: Temperature. Washington, DC. In S. Levitus (Ed.), NOAA Atlas NESDIS 68, U.S. Government Printing Office.
- McCartney, M. S., & Donohue, K. A. (2007). A deep cyclonic gyre in the Australian–Antarctic Basin. *Progress in Oceanography*, 75(4), 675–750. https://doi.org/10.1016/j.pocean.2007.02.008
- Moholdt, G., Padman, L., & Fricker, H. A. (2014). Basal mass budget of Ross and Filchner-Ronne ice shelves, Antarctica, derived from Lagrangian analysis of ICESat altimetry. *Journal of Geophysical Research: Earth Surface*, 119(11), 2361–2380. https://doi.org/10.1002/2014jf003171
- Rignot, E., Jacobs, S. S., Mouginot, J., & Scheuchl, B. (2013). Ice-shelf melting around Antarctica. Science Express, 341, 226–270. https://doi.org/10.1126/science.1235798
- Rintoul, S. R. (1998). On the origin and influence of Adélie Land Bottom Water. Ocean, ice, and atmosphere: Interactions at the Antarctic continental margin, 75, 151–171.
- Snow, K., Rintoul, S., Sloyan, B., & Hogg, A. M. (2018). Change in dense shelf water and Adélie land bottom water precipitated by iceberg calving. *Geophysical Research Letters*, 45(5), 2380–2387. https://doi.org/10.1002/2017gl076195
- Zhang, H., Menemenlis, D., & Fenty, I. (2018). ECCO LLC270 ocean-ice state estimate.

NAKAYAMA ET AL. 10 of 10